Recent Advances and Open Issues on the Use of Smart Bricks for Seismic Monitoring of Masonry Buildings: Experimental Tests and Numerical Simulations

Andrea Meoni(✉), Antonella D'Alessandro, and Filippo Ubertini

Department of Civil and Environmental Engineering, University of Perugia, Via G. Duranti 93, 06125 Perugia, PG, Italy
andrea.meoni@unipg.it

Abstract. Masonry buildings are particularly prone to structural pathologies and brittle failures, typically caused by excessive stresses/strains, differential foundation settlements, aging of materials, and natural hazards, such as seismic events. Monitoring the health state of this type of structures during their service life plays a fundamental role in the identification of incipient damages or critical conditions and the optimization of maintenance interventions. In light of that, the Authors recently developed a novel class of sensors, called smart bricks, for structural health monitoring of masonry constructions. These novel sensors consist of fired bricks made by doping fresh clay with conductive stainless steel micro fibers that enhance the piezoresistive capability of the composite. Smart bricks are equipped with copper plate electrodes and can be deployed within masonry constructions, as normal bricks, for monitoring changes in strain, modifications in load paths, and development of damages. This paper deals with an investigation on the effectiveness of smart bricks for the estimation of strain under increasing compression loads, in particular when sensors are deployed within a typical structural setting. With this aim, smart bricks' strain measurements are compared with those of traditional strain gauges applied onto each tested sample. Furthermore, numerical simulations are carried out for reconstructing strain field maps of a masonry wall subjected to eccentric axial compression tests, by exploiting strain measurements outputted by smart bricks embedded within the load-bearing structure. Overall, results have confirmed the effectiveness of the novel sensors in strain measurements under increasing compression states.

Keywords: Smart bricks · Masonry structures · Structural health monitoring · Smart sensors · Strain sensitivity

1 Introduction

Masonry structures of the European historical and building heritage are a cultural value that must be maintained over time. Nowadays, their preventive conservation is a quite challenging task, since masonry constructions are particularly prone to structural pathologies and fragile collapses mechanisms, owing to excessive stresses/strains,

P. Rizzo and A. Milazzo (Eds.): EWSHM 2020, LNCE 127, pp. 851–860, 2021.
https://doi.org/10.1007/978-3-030-64594-6_82

differential foundation settlements, aging of materials, and natural hazards, such as seismic events [1–3]. In light of that, the employment of tailored Structural Health Monitoring (SHM) systems results in noteworthy benefits for the conservation of masonry constructions during their service life, allowing the real-time identification of changes in the structural behavior of the monitored buildings, thus playing a role of utmost importance in the detection of developing damages or critical conditions, and in planning of retrofitting and maintenance interventions [4–6].

Exploiting their background knowledge in the development of construction materials with self-sensing capabilities for strain monitoring [7, 8], the Authors recently proposed a novel class of sensors, called "smart bricks", for SHM of masonry structures [9, 10]. The new sensing technology consists of fired bricks made by adding electrically conductive stainless steel micro fibers to fresh clay, so as to boost the piezoresistive capability of the base material. Therefore, smart bricks, equipped with external copper plate electrodes, can be internally deployed within masonry constructions as components of the load-bearing structure while monitoring changes in strain, internal redistribution of load paths, and development of damages, through the assessment of variations in their electrical outputs due to changes in their compressive strain state.

The paper investigates the effectiveness of smart bricks in strain estimation when subjected to increasing compression loads. In light of that, tested smart bricks were instrumented with a couple of traditional strain gauges to be used as benchmark. The organization of the rest of the paper is hereinafter reported: Sect. 2 describes the production process of the investigated smart bricks, along with the methodology adopted to conduct electrical measurements. The post-processing of smart bricks' electrical outputs, for strain measurement estimation, is also introduced. Section 3 illustrates the methodologies followed to perform experimental and numerical tests, as well as the achieved results. Section 4 concludes the paper with comments and remarks.

2 The Smart Brick Technology

2.1 Production Process

Smart bricks investigated in this work were produced according to the manufacturing process reported in Fig. 1. Fresh clay was mechanically mixed with electrically conductive stainless steel micro fibers, model R.STAT/S, by considering a filler's content of 0.50% with respect to the weight of fresh clay (Fig. 1a,1b). The obtained composite material was poured within prismatic wooden molds, of $7.0 \times 5.0 \times 5.0$ cm^3, properly wet and sprinkled with sand, to form brick samples (Fig. 1c). The latter were first dried in oven at a temperature of 90 °C for six hours, then fired up to a temperature of 900 °C for another six hours. Smart bricks were finally equipped with two external copper plate electrodes, placed onto their opposite horizontal surfaces with a dry contact, to perform electrical measurements. Each sample was covered with an insulating layer avoiding current flow propagation when inserted within masonry constructions (Fig. 1d).

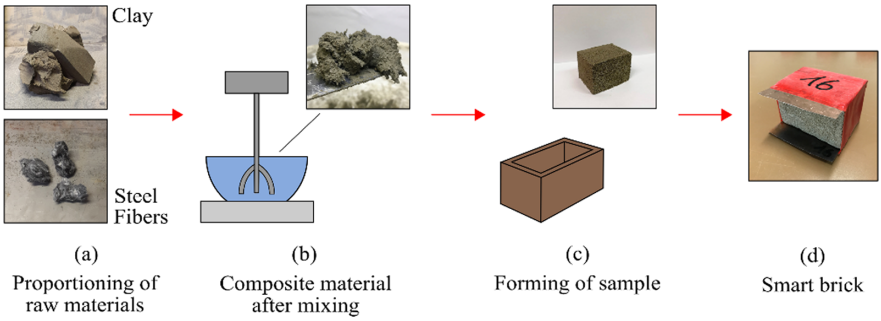

Fig. 1. Illustration of the production process of smart bricks.

2.2 Electrical and Strain Measurements

Smart bricks' electrical measurements were performed by adopting a biphasic DC measurement approach [11]. A voltage square wave input of ±10 V (20 V peak-to-peak), characterized by a duty cycle of 50% and by a frequency of 1 Hz, was applied to each sample by using a function generator, model RIGOL DG1022. The output, a current square wave signal, was measured by means of a digital multimeter, model NI-PXI 4071, mounted within a DAQ, model NI-PXIe 1073, by adopting a sampling frequency of 10 Hz and a current measurement range of 1 μA. Smart bricks' total electrical resistance, R, was calculated according to the Ohm's Law, by considering current intensity measurements taken at the 80% of the positive constant part of the acquired square wave current signal:

$$R(t)|_{t=\hat{t}} = V/I(t)|_{t=\hat{t}} \tag{1}$$

where V is the applied constant voltage in the positive part of the input square wave, equal to +10 V, while I is the value of the current output taken at the time $\hat{t}$.

Smart bricks' strain measurements were retrieved according to a recently proposed theoretical model, called series resistors model, defined by the Authors to describe the strain-sensing behavior of the novel sensors when strained in compression. Such an electromechanical model takes into account both contributions to the sensing due to the enhanced piezoresistivity of the smart bricks and the contact resistance at the electrodes, as follows [12]:

$$\frac{\Delta R}{R_{i,0}} = \frac{R - R_{i,0}}{R_{i,0}} = a'\varepsilon^{-b} - \lambda\varepsilon + c' \cong a'\varepsilon^{-b} - \lambda\varepsilon \tag{2}$$

where $R_{i,0}$ is the unstrained smart bricks' internal electrical resistance, a' represents the relative sensing at the contact resistance, ε is the applied uniaxial strain considered positive in compression, b is the exponential term of the equation ($b = 3$), and λ is the gauge factor. Equation's parameters were determined by applying a properly defined calibration procedure on each smart brick [12]. Once terms of the series resistors model

were determined, strain measurements provided by a smart brick were estimated by post-processing its electrical outputs with Eq. (2).

3 Experimental Investigation

3.1 Axial Compression Tests on Single Smart Bricks

Single smart bricks were tested under increasing axial compression loads to prove their effectiveness in measuring compressive strain by comparing their outputs with those of traditional strain gauges. Therefore, each investigated novel sensor was instrumented with a couple of resistive strain gauges, model Kyowa KFG-20-120-C1-11L1M2R, characterized by a gauge factor of 2.11 and directly attached onto the middle vertical surfaces of the bricks, along the loading direction. A data acquisition card, model NI PXIe-4330, hosted within a chassis NI PXI-1073, was used to acquire measurements from strain gauges, while three Linear Variable Differential Transformers (LVDTs), placed at 120° in plan, were employed to measure displacements for specializing Eq. (2) according to the calibration procedure [12]. The adopted testing setup is reported in Fig. 2, along with the load history applied on each sample.

Figure 3a shows strain histories provided by a tested smart brick, whose strain-sensing behavior has been characterized by setting its series resistors model with the parameters collected in Table 1, and by its corresponding couple of strain gauges, for which the average strain has been considered. Results demonstrate a fairly good match between the compared trends, pointing out a clear strain-sensing capability exhibited by the novel sensor, which detected each increment in the applied load by outputting an increase in its compressive strain state. It should be noted that smart brick's measurements are characterized by a non-linear trend that is attributable to the capability of the novel sensors to take into account settlements of their macro porous structure under compression loads, a mechanical behavior typically exhibited also by the conventional bricks, when strained in compression, since possessing a similar internal structure. Such settlements were induced by the first application of the compression load on the sample, resulting in non-constant increments in its compressive strain under constant increases in the applied load. Further increases in the compressive strain condition of the tested smart brick produced internal settlements of negligible values, hence the novel sensor outputted constant increments in strain at high compressive states. Figure 3b compares sensors' measurements versus an ideal trend, which exemplifies an equal strain-sensing behavior between the considered sensing technologies, thus remarking differences in the nature of their strain outputs. In particular, since the outputs provided by strain gauges are strictly related to the outer portions of the brick where they are punctually attached, rather than to its entire volume, strain gauges' measurements were reasonably less influenced by the internal settlements of the macro porous structure of the brick, as also confirmed by the linear trend characterizing strain gauges' outputs in Fig. 3a.

Table 1. Series resistors model's parameters adopted for computing strain measurements from the smart brick tested to axial compression loads: $R_{i,0}$ is the unstrained smart brick's internal electrical resistance, a' represents the relative sensing at the contact resistance, b is the exponential term of the equation, and λ is the gauge factor.

$R_{i,0}$ [MΩ]	a' [−]	b [−]	λ [−]
5.80	6.86E−12	3.00	363.00

3.2 Small-Scale Masonry Wall Under Eccentric Axial Compression Load

A small-scale masonry wall specimen, equipped with seven smart bricks, was subjected to eccentric axial compression tests to investigate the effectiveness of the novel sensors in measuring strain under compression loads when embedded within a structural setting. The specimen, a wall of 37.0 × 5.0 × 39.0 cm^3 composed by bricks arranged in seven rows and five columns with mortar layers of thickness of about 0.5 cm (Fig. 4a), was tested by applying on its right side the load history reported in Fig. 4b, considering a distance of about 11 cm from its centerline. Smart bricks were fully integrated within the thickness of the tested structural element as exemplified in Fig. 5a, which also illustrates the cracking pattern visually detected after completing the test. It should be noted that cracks named c_1, c_2, and c_3 were formed at the load step of 15 kN, while cracks c_4 and c_5 were developed after the application of the load steps of 25 and 50 kN, respectively. Formed cracks got larger while conducting the tests as the applied load increased. A couple of traditional strain gauges was attached onto each embedded sensor by allowing the comparison between strain measurements. These last were estimated from smart bricks' electrical outputs by using Eq. (2) set with the equation's parameters collected in Table 2 and obtained by considering the average value of each coefficient of the equation determined by testing a broader set of smart bricks made with a content of microfibers of 0.50%, while the average strain was considered for each couple of strain gauges, whose outputs were gathered through a DAQ, model IMC Cronos-PL 16, set with a nominal gauge resistance of 120 Ω.

Figure 5b reports changes in strain versus applied load for smart brick 3 and its corresponding couple of strain gauges, for which the average strain has been considered. The application of the load on the wall specimen produced marked changes in the strain state of the considered smart brick until the load step of 15 kN, after which the increasing trend indicating increments in compressive strain provided by the novel sensor was interrupted in correspondence to the formation of cracks c_1, c_2, and c_3, which induced a first load paths redistribution internally to the tested structural element. On the other hand, strain gauges recorded increasing changes in strain up to the load step of 50 kN, after which, conceivably, the opening of crack c_1 was of such severity to induce an internal load redistribution that deviated compressive stresses from the outer surfaces of the smart brick 3 where the couple of strain gauges was attached. The traditional sensors recorded a decrease in compressive strain even if the load applied on the specimen was increased up to 60 kN.

Measurements acquired from smart bricks and strain gauges were further post-processed to map the strain field throughout the wall specimen by using the Ordinary Kriging method, a statistical tool for data spatial interpolation [13]. Figure 6 shows maps of changes in strain computed for the load steps corresponding to applied loads of 10 and 60 kN, respectively. Plotted maps are consistent with the performed eccentric axial compression test since they highlight the right part of the wall as the most strained in compression due to the direct application of the load. It is worth noting that maps retrieved by spatially interpolating smart bricks' strain measurements denote that the novel sensors, being internally deployed in the thickness of the wall specimen, were capable of revealing a more uniform internal redistribution of the applied load than strain gauges, which were less sensitive to changes in strain since externally attached to the tested structural element.

Table 2. Series resistors model's parameters adopted for computing strain measurements from smart bricks embedded within the small-scale masonry wall specimen: $R_{i,0}$ is the unstrained smart bricks' internal electrical resistance, a' represents the relative sensing at the contact resistance, b is the exponential term of the equation, and λ is the gauge factor.

$R_{i,0}$ [MΩ]	a' [−]	b [−]	λ [−]
7.92	5.86E−12	3.00	397.00

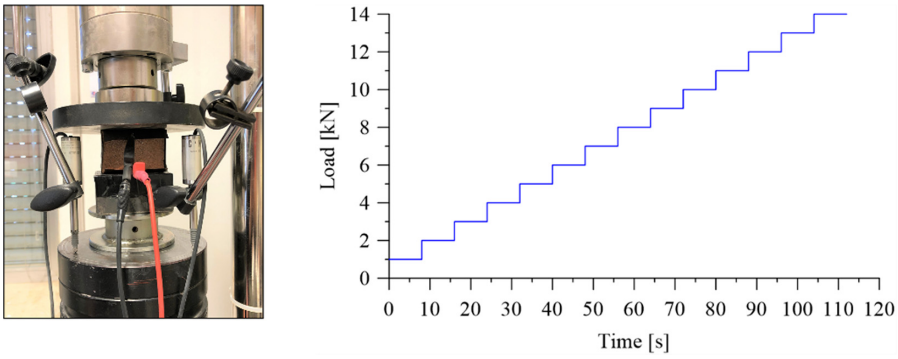

Fig. 2. Testing setup and load history adopted to perform axial compression tests on single smart bricks instrumented with a couple of traditional strain gauges.

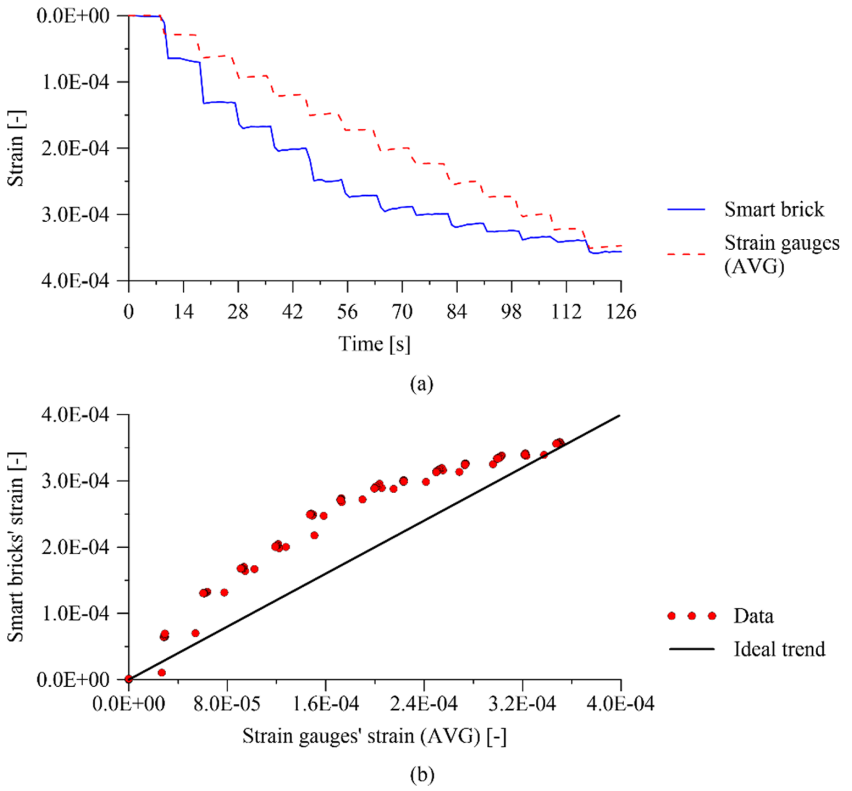

Fig. 3. Results obtained by performing axial compression tests on a smart brick instrumented with a couple of traditional strain gauges, for which the average strain (AVG) was taken into account: (a) Outputted strain histories; (b) Direct comparison between smart brick's and strain gauges' measurements versus an ideal trend.

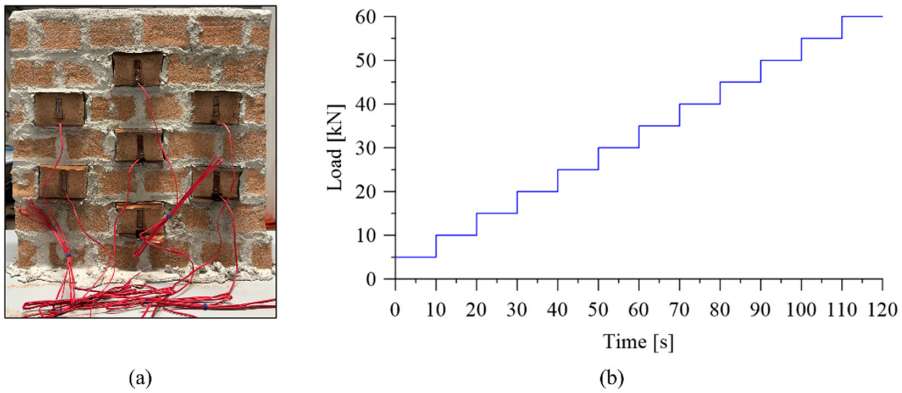

Fig. 4. Eccentric axial compression tests on a small-scale masonry wall specimen: (a) Picture of the tested structural element; (b) Applied load history.

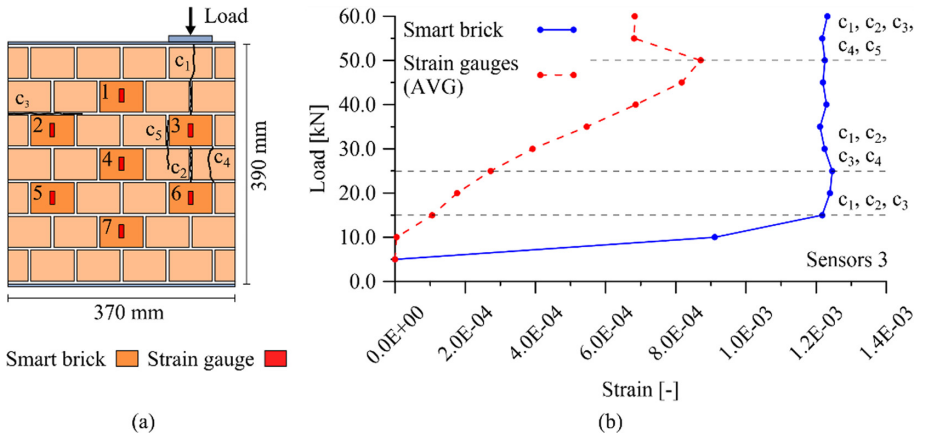

Fig. 5. Results from the eccentric axial compression tests on a small-scale masonry wall specimen: (a) Smart bricks and strain gauges deployment with annotated the cracking pattern detected at the end of the test; (b) Changes in strain versus applied load for smart brick n. 3 and its couple of strain gauges, for which the average strain (AVG) was taken into account.

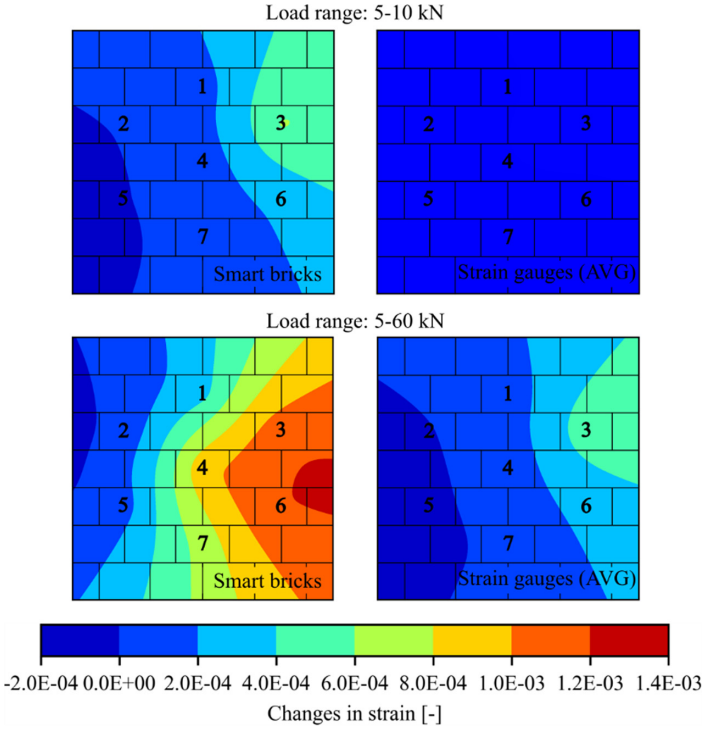

Fig. 6. Strain field maps of the small-scale masonry wall specimen reconstructed by interpolating measurements provided by smart bricks and traditional strain gauges, for which the average strain (AVG) was taken into account, through the Ordinary Kriging interpolator (1–7 represent the position of the smart bricks).

4 Conclusions

The paper has presented experimental and numerical investigations on the effectiveness of smart bricks for the estimation of strain under compression loads. Therefore, the strain-sensing capability of the novel sensors, made with a stainless steel microfibers' content of 0.50% with respect to the weight of fresh clay, was assessed, first, by applying an increasing axial compression load on single samples, and then, by employing smart bricks for monitoring the strain state of a small-scale masonry wall specimen subjected to eccentric axial compression loads. A couple of traditional strain gauges were attached onto the outer surfaces of each novel sensor, thus allowing the comparison between strain measurements.

Results obtained by carrying out axial compression tests on single smart bricks have demonstrated a clear strain-sensing capability of the novel sensors to compressive strains, by also highlighting some differences in the nature of the measurements outputted by the compared sensing technologies, which were however consistent between them. Indeed, smart bricks have shown an enhanced strain-sensitivity also capable of reproducing the non-linear mechanical behavior typically exhibited by the conventional bricks when strained in compression, since their internal macro porous structure is similar and prone to settlements under low compressive state.

Results collected by performing eccentric axial compression tests on a small-scale masonry wall specimen have demonstrated the usefulness of smart bricks in revealing the internal load paths redistributions that occurred on the wall specimen due to the increasing applied load and consequent cracks formations, in comparison with traditional strain gauges. These last, in particular, being externally and punctually attached, were less sensitive to the internal stress modifications. Moreover, numerical results achieved by using the Ordinary Kriging interpolator for the reconstruction of the strain field maps of the wall specimen have shown the effectiveness of the novel sensor for mapping concentrations/relaxations in the strain field of masonry structural elements.

Overall, obtained results have demonstrated that smart bricks are effective in strain estimation under compression loads, thus confirming the novel sensors as a powerful new sensing technology tailored for SHM of masonry structures.

Acknowledgements. This work was supported by the Italian Ministry of Education, University and Research (MIUR) through the founded project of Relevant National Interest (PRIN) "DETECT-AGING (Degradation Effects on sTructural safEty of Cultural heriTAGe constructions through simulation and health monitorING)" (Protocol no. 201747Y73L). The first author also wishes to acknowledge the German Academic Exchange Service (DAAD) for partially supporting his Ph.D. through the founded project of Research Grants – Short-Term Grants, 2019 (57442045).

References

1. Lagomarsino, S.: On the vulnerability assessment of monumental buildings. Bull. Earthq. Eng. **4**, 445–463 (2006)
2. De Lorenzis, L., DeJong, M., Ochsendorf, J.: Failure of masonry arches under impulse base motion. Earthq. Eng. Struct. Dyn. **36**(14), 2119–2136 (2007)

3. Atamturktur, S., Bornn, L., Hemez, F.: Vibration characteristics of vaulted masonry monuments undergoing differential support settlement. Eng. Struct. **33**(9), 2472–2484 (2011)
4. Masciotta, M.G., Roque, J.C., Ramos, L.F., Lourenço, P.B.: A multidisciplinary approach to assess the health state of heritage structures: the case study of the Church of Monastery of Jerónimos in Lisbon. Constr. Build. Mater. **116**, 169–187 (2016)
5. Gentile, C., Saisi, A.: Ambient vibration testing of historic masonry towers for structural identification and damage assessment. Constr. Build. Mater. **21**(6), 1311–1321 (2007)
6. Carpinteri, A., Lacidogna, G.: Damage monitoring of an historical masonry building by the acoustic emission technique. Mater. Struct. **39**(2), 161–167 (2006)
7. D'Alessandro, A., et al.: Static and dynamic strain monitoring of reinforced concrete components through embedded carbon nanotube cement-based sensors. Shock Vibr. **2017** (2), 1–11 (2017)
8. Meoni, A., et al.: An experimental study on static and dynamic strain sensitivity of embeddable smart concrete sensors doped with carbon nanotubes for SHM of large structures. Sensors **18**(3), 831 (2018)
9. D'Alessandro, A., Meoni, A., Ubertini, F.: Stainless steel microfibers for strain-sensing smart clay bricks. J. Sens. **2018**, 1–8 (2018)
10. Meoni, A., D'Alessandro, A., Cavalagli, N., Gioffré, M., Ubertini, F.: Shaking table tests on a masonry building monitored using smart bricks: damage detection and localization. Earthq. Eng. Struct. Dyn. **48**(8), 910–928 (2019)
11. Downey, A., D'Alessandro, A., Ubertini, F., Laflamme, S., Geiger, R.: Biphasic DC measurement approach for enhanced measurement stability and multi-channel sampling of self-sensing multi-functional structural materials doped with carbon-based additives. Smart Mater. Struct. **26**(6), 065008 (2017)
12. Meoni, A., D'Alessandro, A., Ubertini, F.: Characterization of the strain-sensing behavior of smart bricks: A new theoretical model and its application for monitoring of masonry structural elements. Constr. Build. Mater. **250**, 118907 (2020)
13. Cressie, N.: Spatial prediction and ordinary kriging. Math. Geol. **20**(4), 405–421 (1988)